A Multiple Specimen Test Technique To Determine Fatigue Crack Growth Rates for Conditions Relevant to Offshore Structures

Principal Investigator: William H. Hartt
Florida Atlantic University
Department of Ocean Engineering
Laboratory of Materials
Boca Raton, FL 33431

Objective: — To develop an experimental technique whereby fatigue properties of newly developed higher strength steels, as are critical to deep water structural concepts, can be more rapidly and efficiently evaluated, and to use the technique to determine the influence of steel composition and microstructure potential and stress ratio on crack propagation behavior of these steels in natural seawater.

Fatigue of structural and equipment components fabricated from high strength steels is a potential problem for deep water offshore structures which typically undergo alternate loading of high mean stress and low frequencies and are subjected to a corrosive environment. A conservative approach to determining fatigue resistance considers a cracked material and the propagation of that crack under relevant environment and alternate loading conditions (fracture mechanics approach).

Loading on a cracked structure induces a concentrated stress field in the vicinity of the crack tip that within certain limitations can be evaluated by linear elastic fracture mechanics. Such a stress state is a function of the nominal stress, crack size and geometry of the structure or component. The stress field is characterized by three stress intensity factors K_I, K_{II} and K_{III}, where each addresses a particular mode of loading (mode I, II or III). Figure 1 illustrates these three different crack propagation modes, and any loading situation may be represented by some combination of these.

When the structure or component is alternately loaded, these factors exhibit a maximum and minimum value corresponding, respectively, to the maximum and minimum stress applied. It is therefore possible to define three stress intensity factor ranges ΔK_I, ΔK_{II} and ΔK_{III}. Figure 2 gives an example of the variations with time of an alternate loading and the corresponding K_{max}, K_{min} and ΔK values.

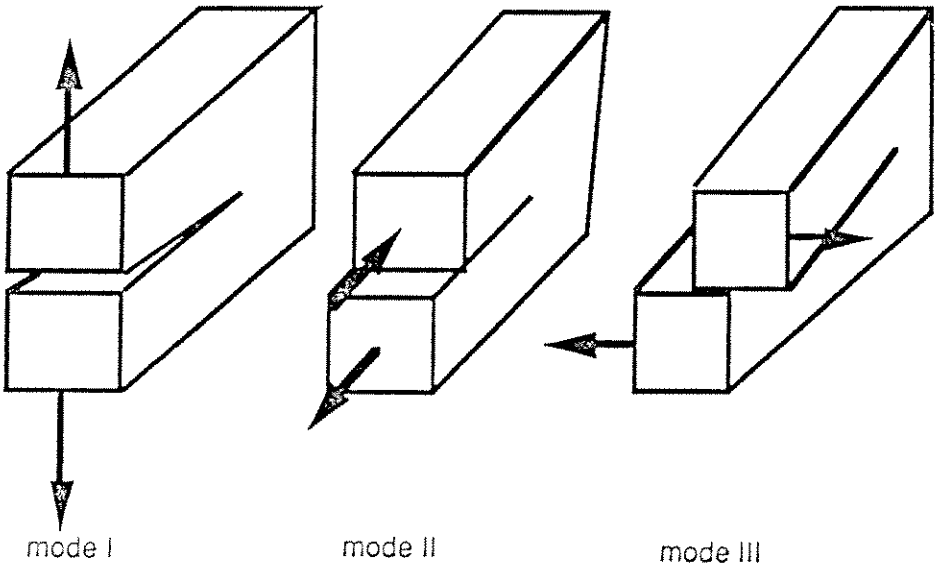

Figure 1—Modes of Crack Propagation.

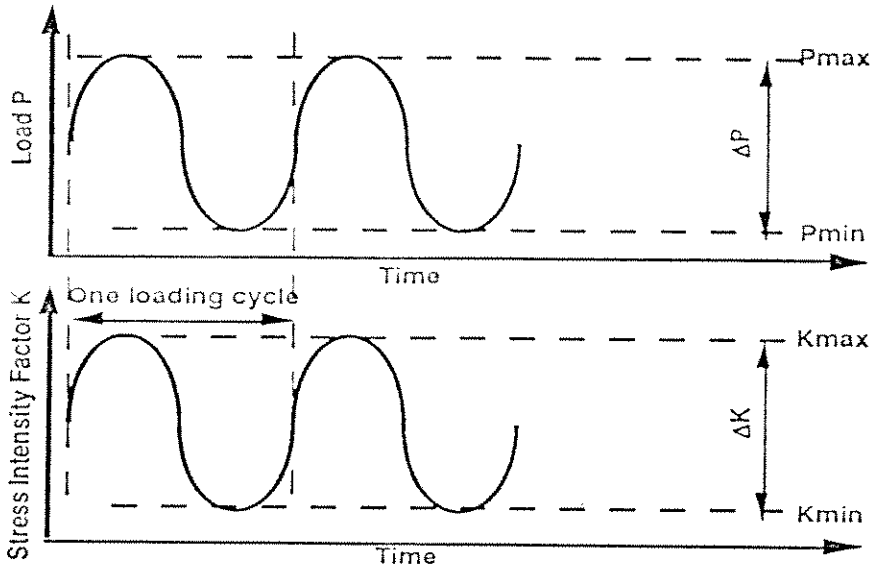

Figure 2—Variations of Load P and Stress Intensity Factor K With Time.

Experiments relate crack growth rate da/dN (crack length increment per loading cycle) to ΔK_I, ΔK_{II} and ΔK_{III} for some specific environmental condition. Figure 3 shows a da/dN-ΔK_I plot for ASTM A533 B1 steel tested in ambient room air at 24°C (Paris and others, 1972). It is observed that in mode I fatigue data show a strong dependence of crack growth rate da/dN on ΔK_I, and there exists a threshold stress intensity range ΔK_{Ith} below which crack growth does not occur. ΔK_{Ith} is an important parameter for determining if a preexisting crack in a structure will or will not propagate.

Only limited threshold fatigue data have been developed for high strength steels in environments relevant to offshore applications. This is a consequence of the time consumed by any corrosion fatigue experiment performed at a low frequency. For example, at a rate of 10^{-7} mm/cycle and a cycling frequency of 0.1 Hz, it takes more than three years for the crack length to increase by 1 mm. For that reason a new experimental approach has been developed whereby near-threshold fatigue crack growth rates for several specimens loaded in series are simultaneously determined.

The analytical part of the study involved the design of a new specimen geometry. During the experiments crack length is monitored by the DCPD (Direct Current Potential Drop) technique, whereby the potential drop across the crack plane in association with a constant current flowing in the specimen is measured. The calibration relationship between potential drop and crack length was computed for the new specimen geometry. This project has now reached the experimental phase, and the analytical results for the new specimen geometry have been verified, and different high strength steels are now being tested in air and seawater.

DESIGN OF A NEW SPECIMEN GEOMETRY

For a specimen of constant thickness, B, the stress intensity factor K is proportional to applied load P and inversely proportional to B, as expressed by

$$K = \frac{P}{B} f(\text{geometric parameters}) \quad (1)$$

or

$$\Delta K = \frac{\Delta P}{B} f(\text{geometric parameters}). \quad (2)$$

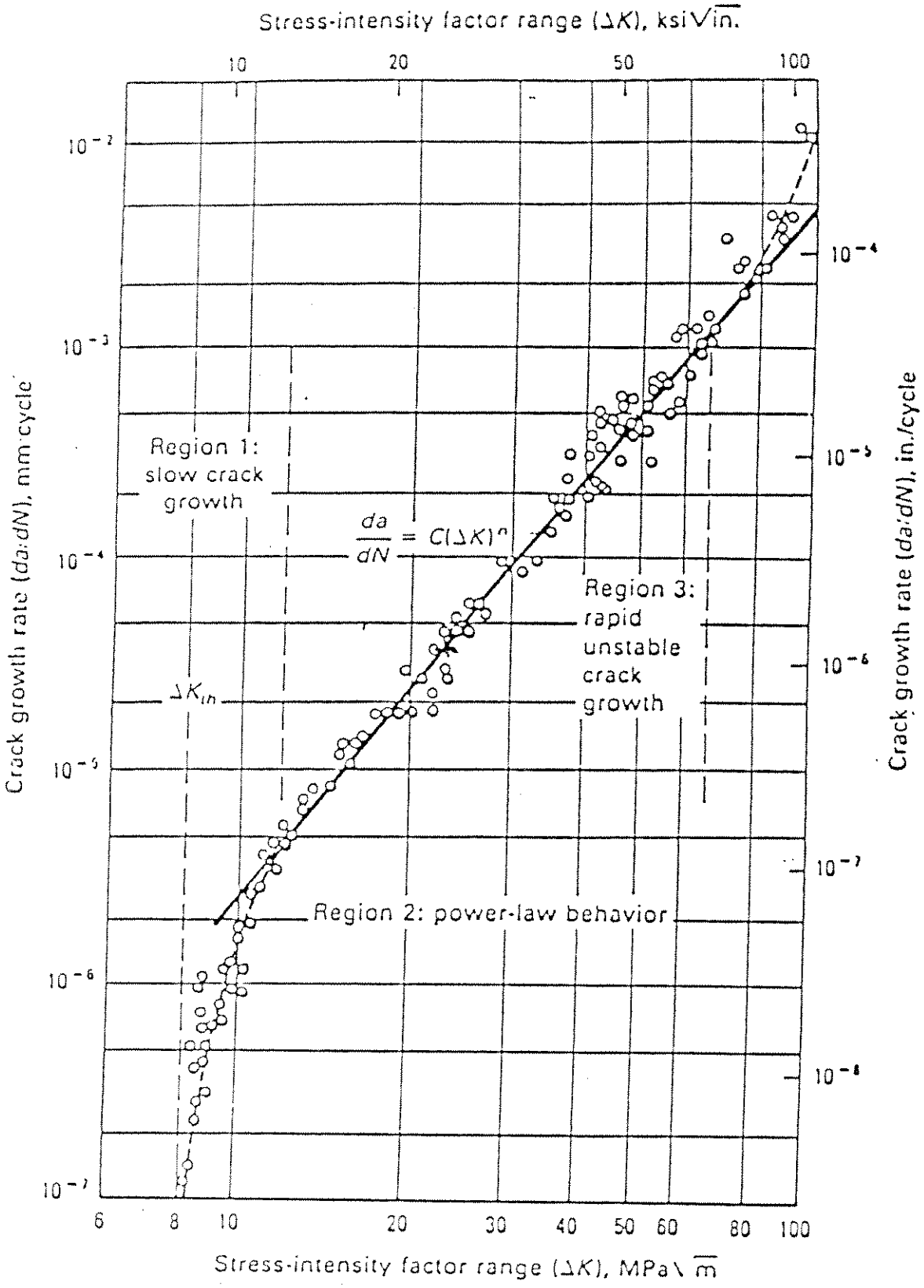

Figure 3—Fatigue Crack Growth Behavior of ASTM A533 B1 Steel.

Among the geometric parameters are crack length a and specimen width and height. The functional dependence is only upon a with different alternatives illustrated by Figure 4. For example, in the case of the C-T specimen shown in Figure 5, K is an increasing function of crack length as illustrated in Figure 6.

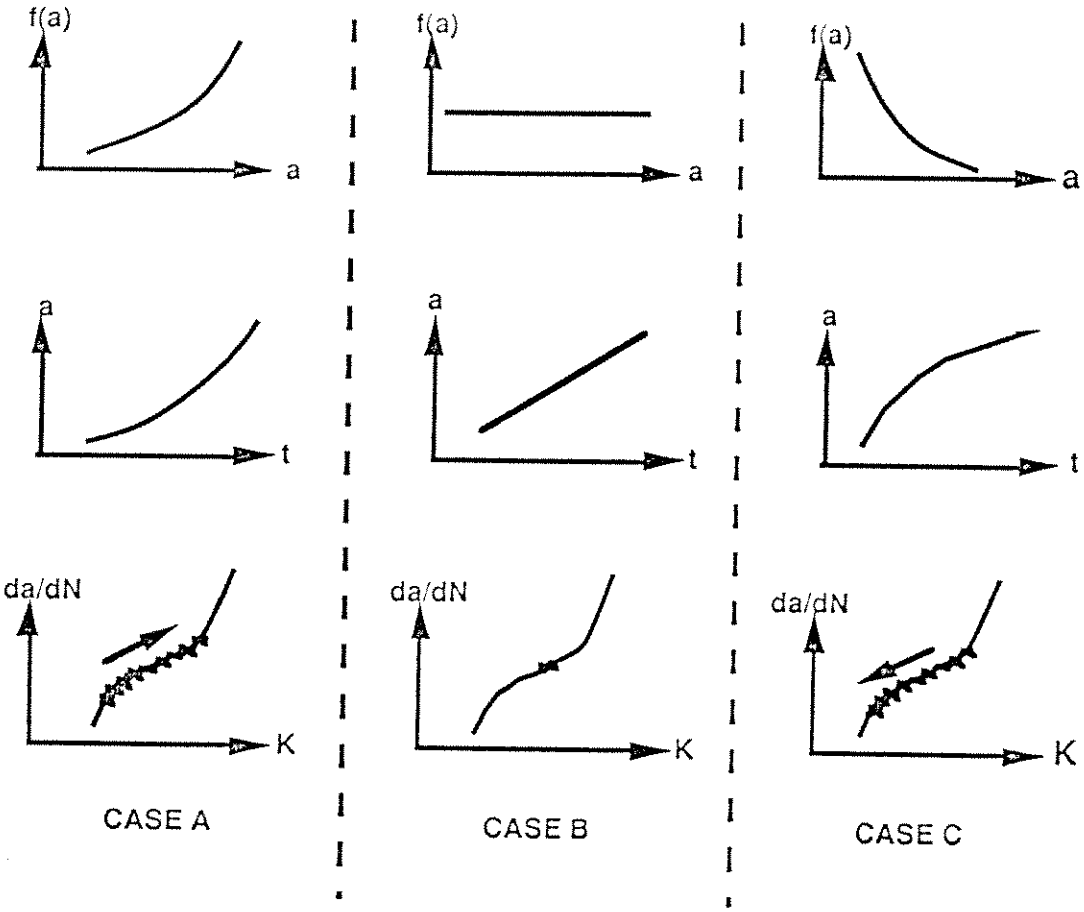

Figure 4—Modes of Crack Propagation at Constant Load Amplitude.

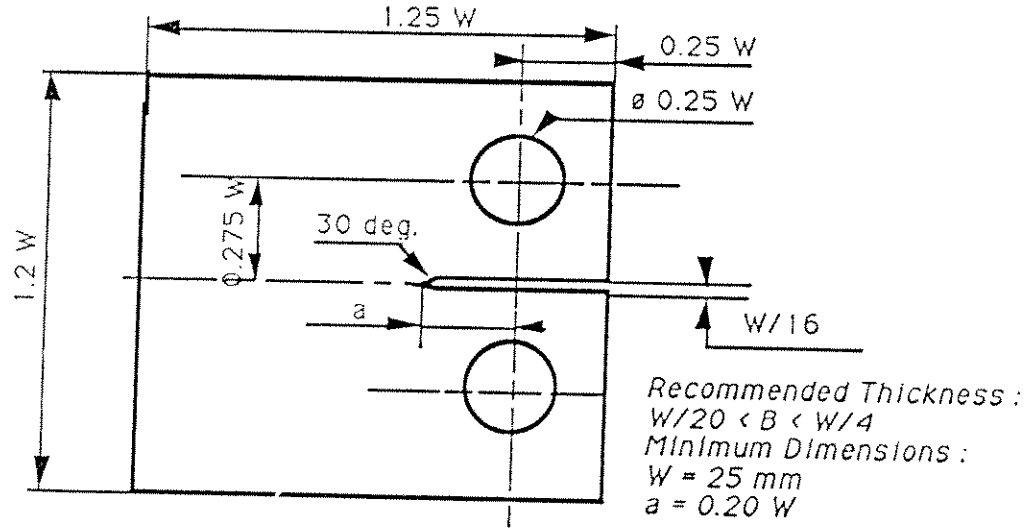

Figure 5—Compact-Tension Specimen Geometry.

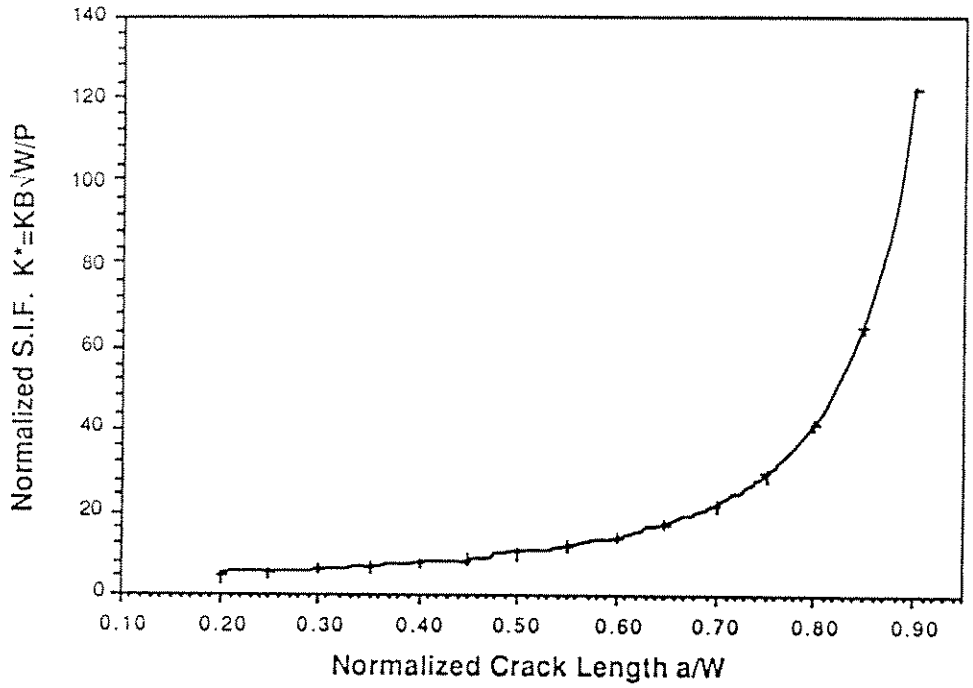

Figure 6—Relation Between Normalized Stress Intensity Factor and Normalized Crack Length for a C-T Specimen.

The use of several compact-tension specimens tested in series is inappropriate for investigating crack growth behavior, since stress intensity factor increases with increasing crack length (constant load amplitude or range), and this dictates load shedding according to the specimen for which crack propagation is most rapid. Stress intensity factor range for the remaining specimens (smaller crack length) consequently decreases to low values and may even fall to below ΔK_{Ith}, such that little or no information is obtained from them. Development of a specimen corresponding to case C of Figure 4, for which at constant load amplitude ΔK decreases with increasing crack length, was an objective of this study. Figure 7 presents one half of the geometry of the tapered specimen that was designed by finite element analysis. As shown in Figure 8, this tapered specimen is K-decreasing for 44 mm < a < 90 mm.

Such a specimen must have side-grooves to keep the crack propagation stable (that is, for the crack to be maintained in the center plane). Thickness at the side-groove position (crack plane), B_n, was determined experimentally, and it was determined that $B_n/B = 0.70$ was appropriate. From the stress intensity factor K previously computed without side-groove, the stress intensity factor K′ for the same specimen with side-grooves can be deduced from the relation

$$K' = \frac{K}{\sqrt{\frac{B_n}{B}}} \tag{3}$$

The specimen crack starter notch was fabricated by Electro-Discharge Machining (EDM) using a 0.5 mm diameter wire which gave a tip radius of approximately 0.25 mm, as determined by ASTM Standard E647 in the particular case of high strength steels (ASTM, 1986).

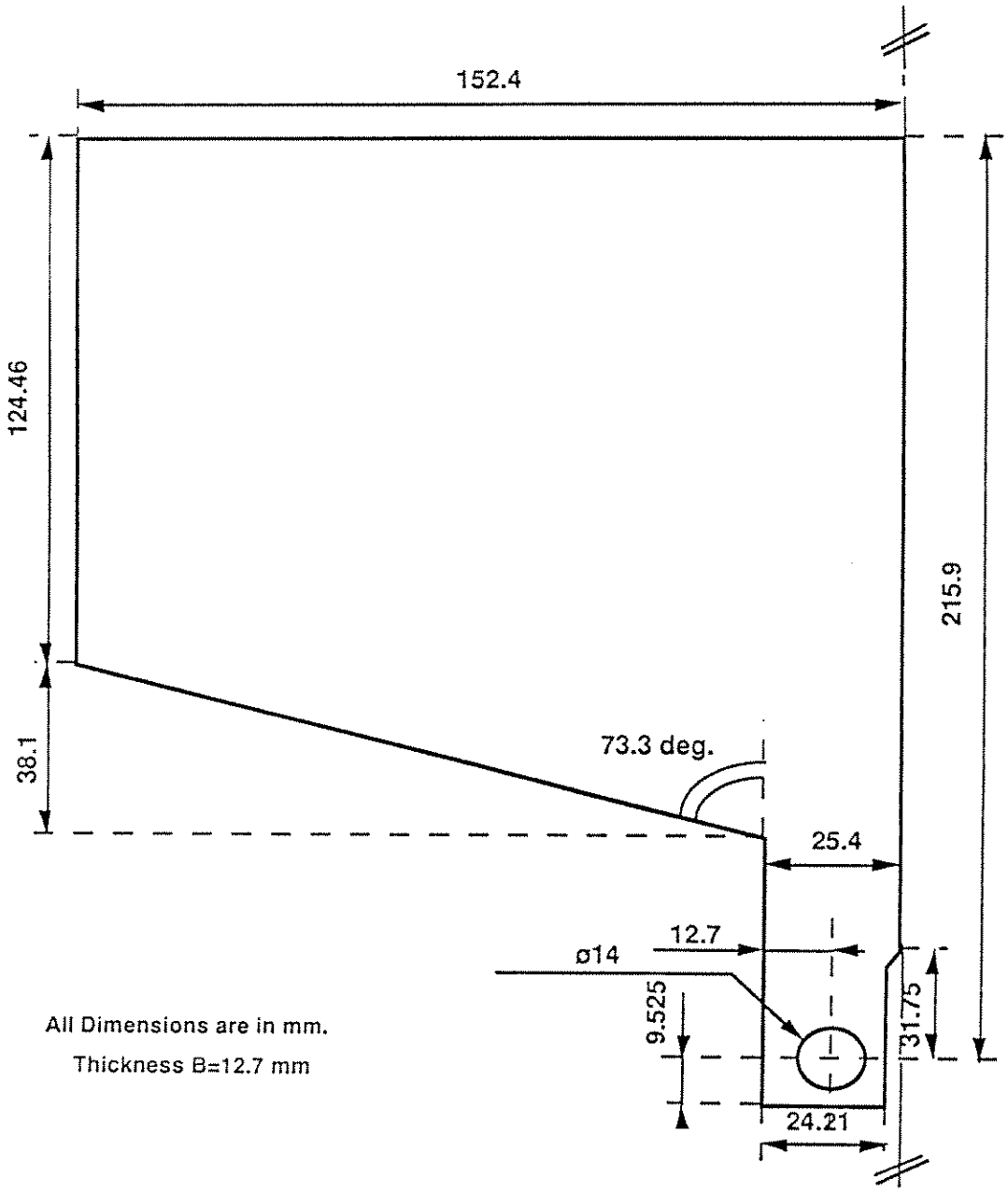

Figure 7—Proposed Test Specimen Geometry (One Half).

Determination of Crack Length by the DCPD Technique

Crack length determination from electric potential measurements relies on the principle that the electrical field in a specimen with a current flowing through it is a function of geometry, including crack length. Therefore, potential drop between two points can be related to crack length through calibration or analytical (or both) relationships (Johnson, 1965; Schwalbe and Hellman, 1981; Hicks and Pickard, 1982). Either direct current (DC) or alternating current (AC) techniques can be used to measure the crack length of a specimen (Watt, 1980). Only the direct current method was considered here, and the calibration relationship determination is explained below.

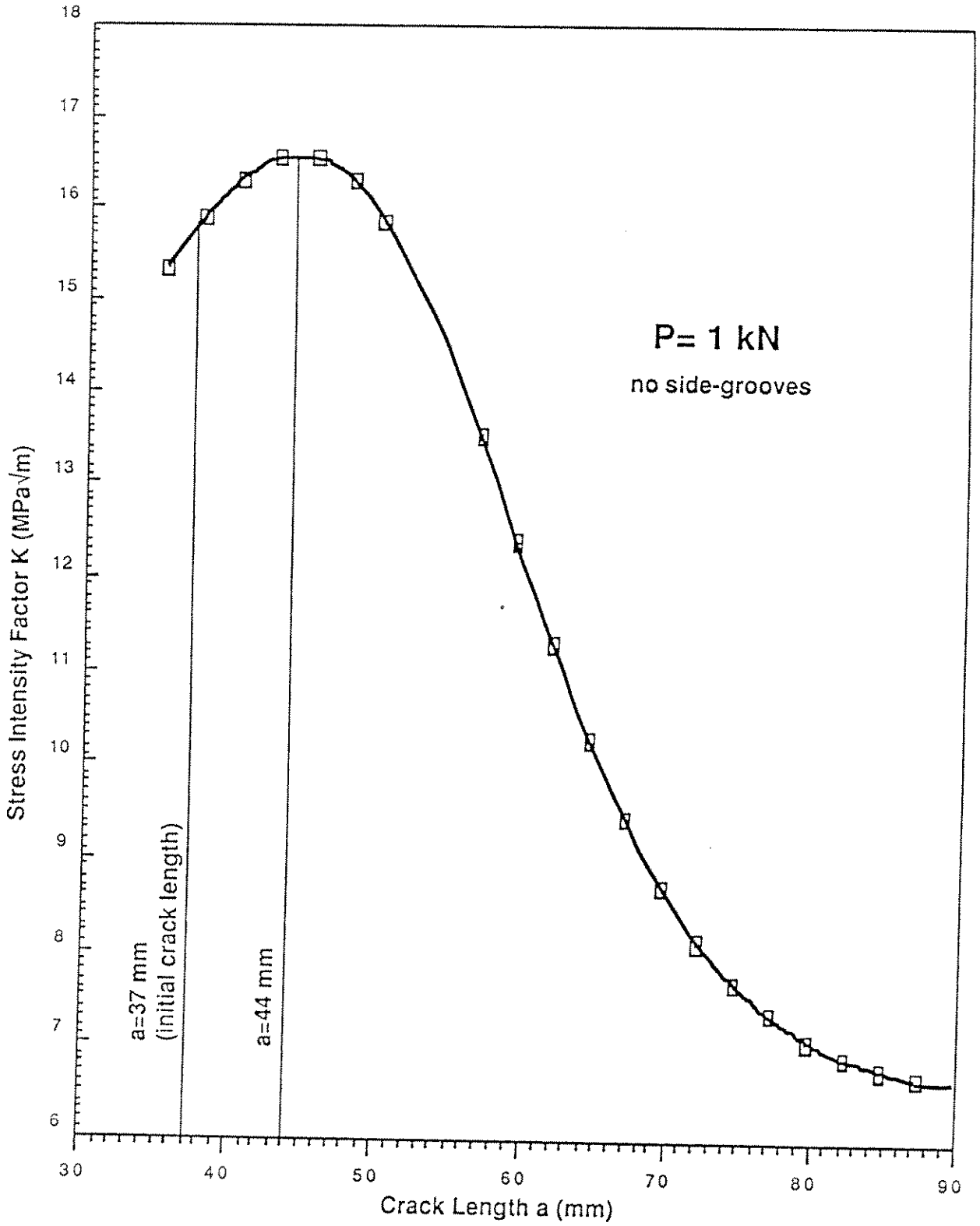

Figure 8—Relation Between Stress Intensity Factor and Crack Length for the New Specimen Geometry.

Figure 9 illustrates the potential and current lead locations for the proposed specimen geometry shown in Figure 7. The electrical potential drop across the crack plane is measured; and as the crack propagates, the resistance and, hence, the measured pd increases due to the reduction in uncracked cross sectional area. As the thickness is small compared to the width and height and as the specimen is symmetric with respect to the crack plane, the equipotential distribution is two-dimensional and has the configuration shown in Figure 10.

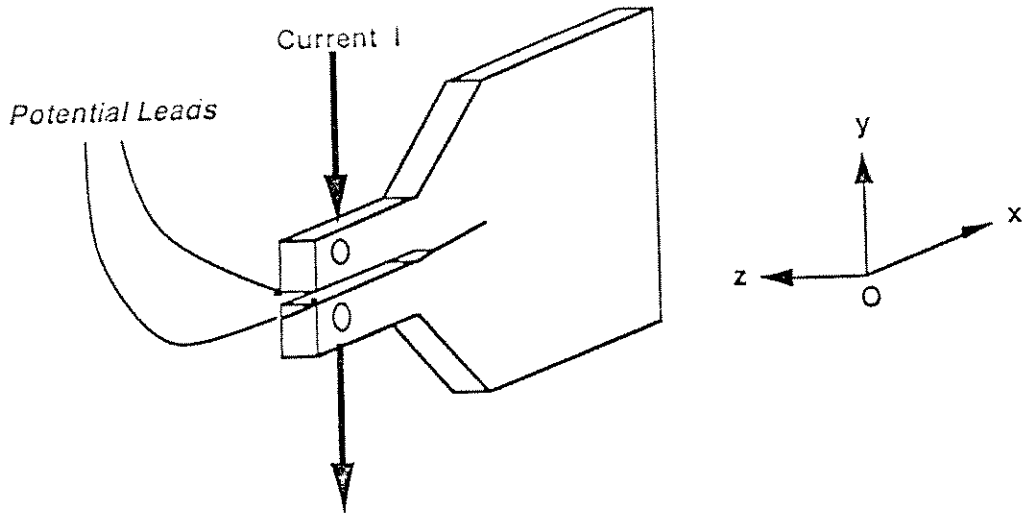

Figure 9—Potential and Current Lead Locations.

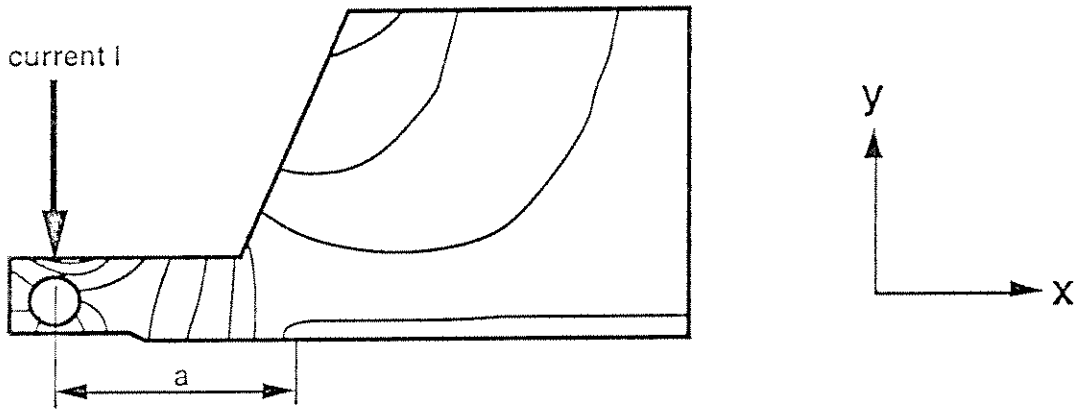

Figure 10—Equipotential Distribution.

Calibration Relationship

For a given geometry, current input and potential lead locations, potential drop V across the crack plane depends on 1) crack length *a*. 2) current I (V is proportional to 1), 3) material conductivity *k* (V is inversely proportional to k). Consider potential V_0 corresponding to a certain crack length a_0. V/V_0 does not depend on I and k but only on crack length *a*. The relation $a = f(V/V_0)$ can consequently be obtained by finite element analysis and is used to determine crack length *a* by measuring the potential drop across the crack plane. The calibration curve for the presently developed specimen is shown in Figure 11.

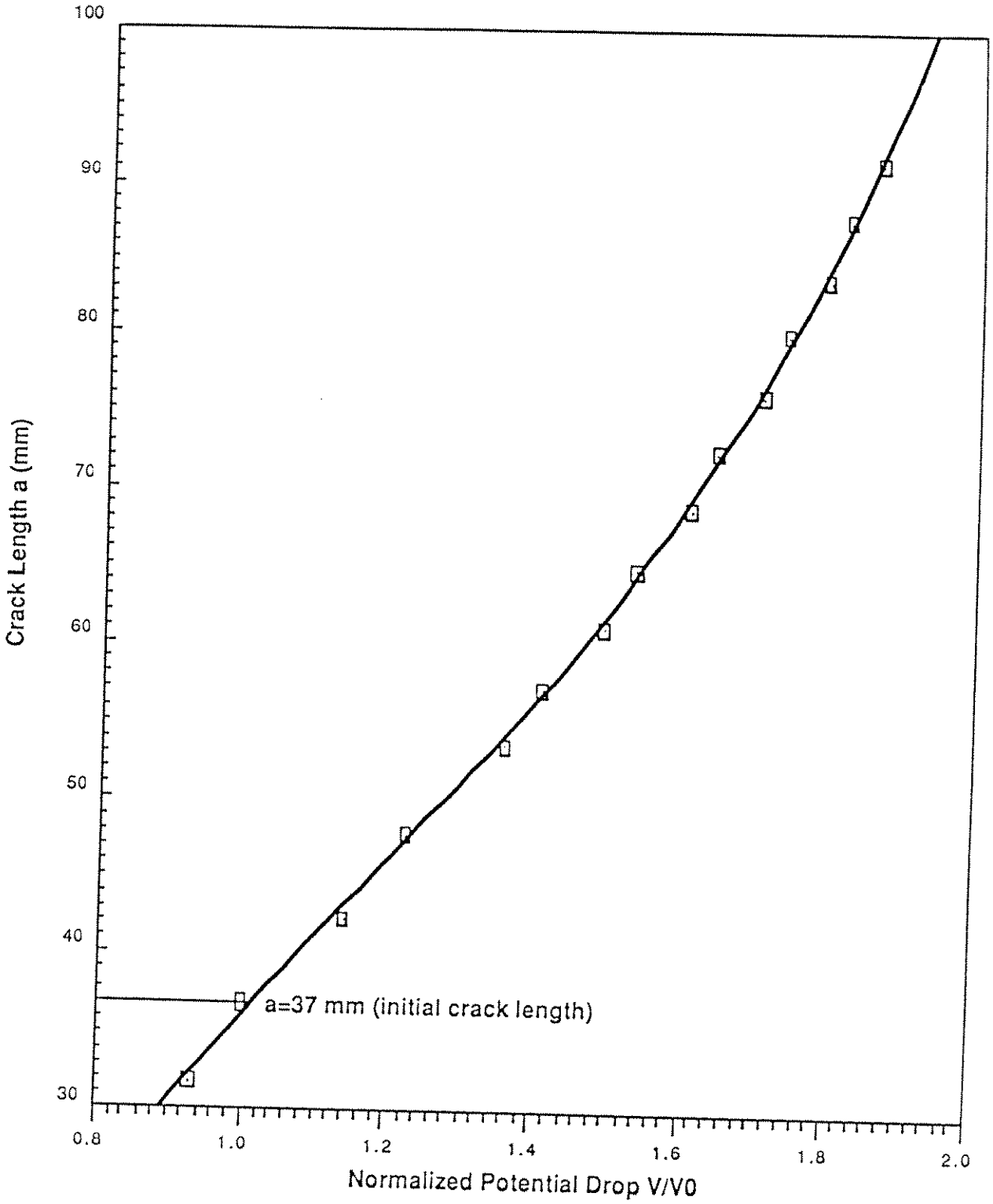

Figure 11—Relation Between Crack Length and Normalized Potential Drop for the Proposed Specimen Geometry.

Accuracy of Crack Length Determination

Accuracy of electrical potential measurements of crack length is limited by a number of factors including the electrical stability and resolution of the potential measurement system, temperature changes which influence electrical conductivity and electrical contacts between crack surfaces. To minimize crack length measurement error due to temperature fluctuations, two specimens (active and reference) of the same material are exposed to the same environmental conditions as shown by Figure 12, with the active specimen tested in fatigue.

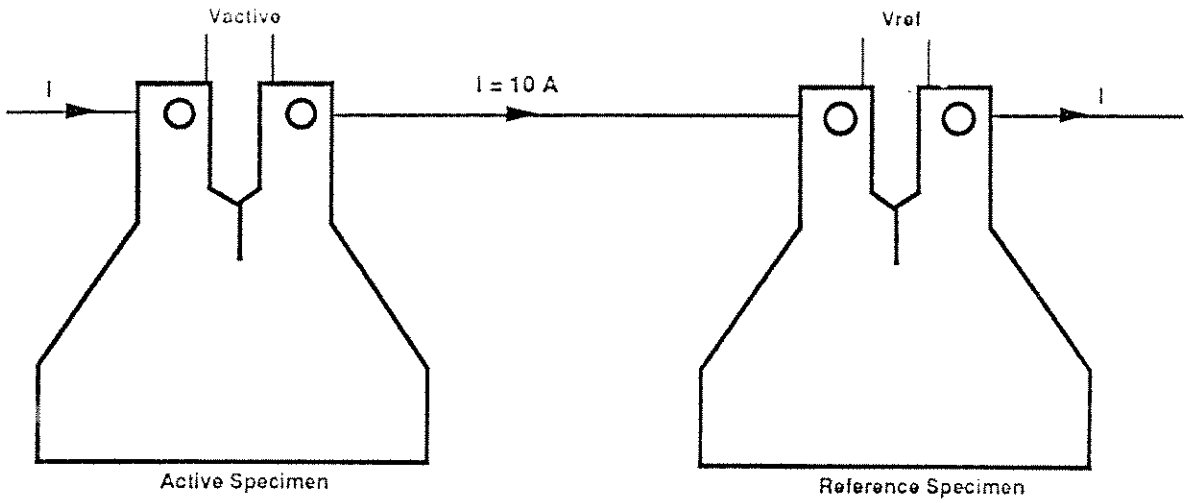

Figure 12—Temperature Fluctuation Correction.

If conductivity k of the two specimens is modified by temperature fluctuations during the experiment and becomes k', two new potential drops are obtained from the relations

$$V'_{ref} = V_{ref}\frac{k}{k'} \text{ and} \tag{4}$$

$$V'_{active} = V_{active}\frac{k}{k'} \, . \tag{5}$$

The corrected potential drop

$$V_{cor} = \frac{V_{active}\,V_{ref}}{V'_{ref}} \tag{6}$$

remains constant if the two specimens undergo the same conductivity variations.

Before the alternate loading starts the reference potential V_{ref} and the initial potential V_0 must be determined. These are measured over a two day period, and the mean values and standard deviations are computed, which gives an order of magnitude estimate of potential measurement accuracy. During the fatigue experiment the ratio V_{cor}/V_0 is used to compute crack length. However, asperities on the mating crack faces can come in contact and introduce an error in the measurement of crack length by the DCPD technique, and so a technique involving post-test calibration, based upon optical measurements on the crack face, must be included.

EXPERIMENTAL SET-UP

The experimental set-up developed for corrosion fatigue tests on several specimens loaded in series is based on two specially configurated, multiple station frames and a DCPD data acquisition system. Each frame is operated in conjunction with a MTS actuator, closed-loop servo hydraulic control system. Figure 13 is a photograph of one frame with five specimens under test, and a schematic of the overall testing system is shown in Figure 14. A constant current I = 10 A supplied by the DC current source is flowing through fourteen specimens: twelve tapered specimens and two short-crack bend specimens. Six tapered specimens are loaded in series on Frame #1 (Specimens #1 to #6), five on Frame #2 (Specimens #7 to #11), and one of the two short-crack specimens is loaded by a third actuator (Specimen #12). The two remaining specimens, a tapered specimen (Reference #1) and a short-crack specimen (Reference #2) are unloaded and used as reference specimens as previously described. The macro-cracks are the subject of the present research project, whereas the short-cracks are addressed by another project conducted in parallel.

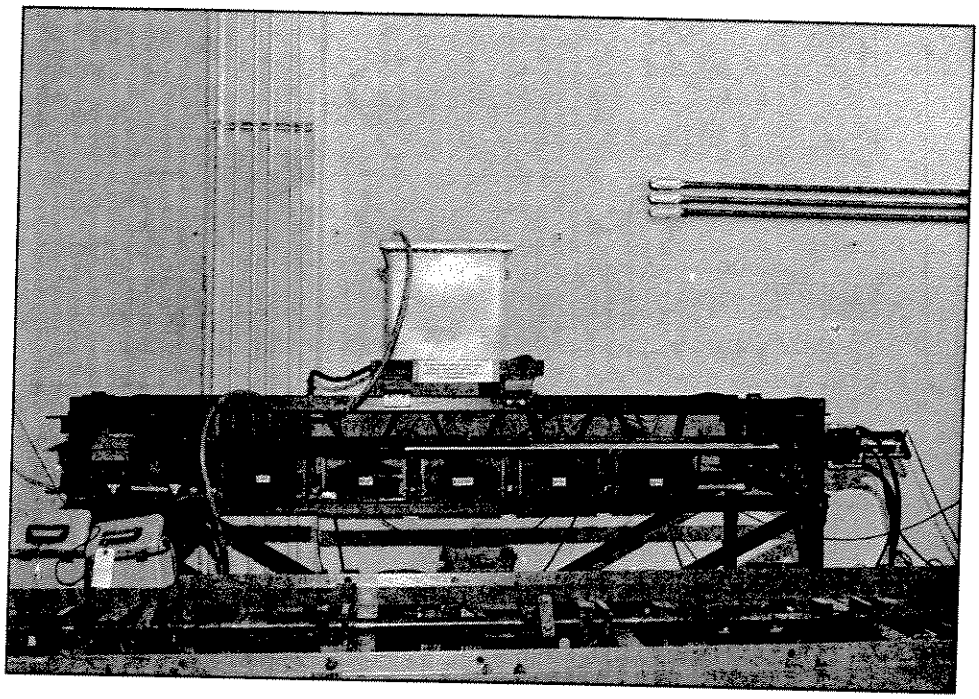

Figure 13—Photograph of Frame #2 With Five Specimens Under Test.

EXPERIMENTAL VERIFICATION OF THE ANALYTICAL EXPRESSIONS K = f(a) AND a = f(V/V$_0$)

Several tapered and classic compact-tension specimens fabricated from a 12.7 mm thick plate of 1018 cold rolled steel were tested in air to confirm appropriateness of the procedure and the relation between crack length and potential drop and between stress intensity factor and crack length.

Relation between stress intensity factor and crack length (Figure 8) and Equation 3 were verified by comparing under the same loading conditions crack growth rates obtained from a tapered specimen and from a classic C-T specimen. Figure 15 shows crack growth rates measured on the two specimen types. An excellent correlation between the two sets of data is observed. It has been concluded that the proposed specimen provides a satisfactory approach to fatigue crack growth rate testing.

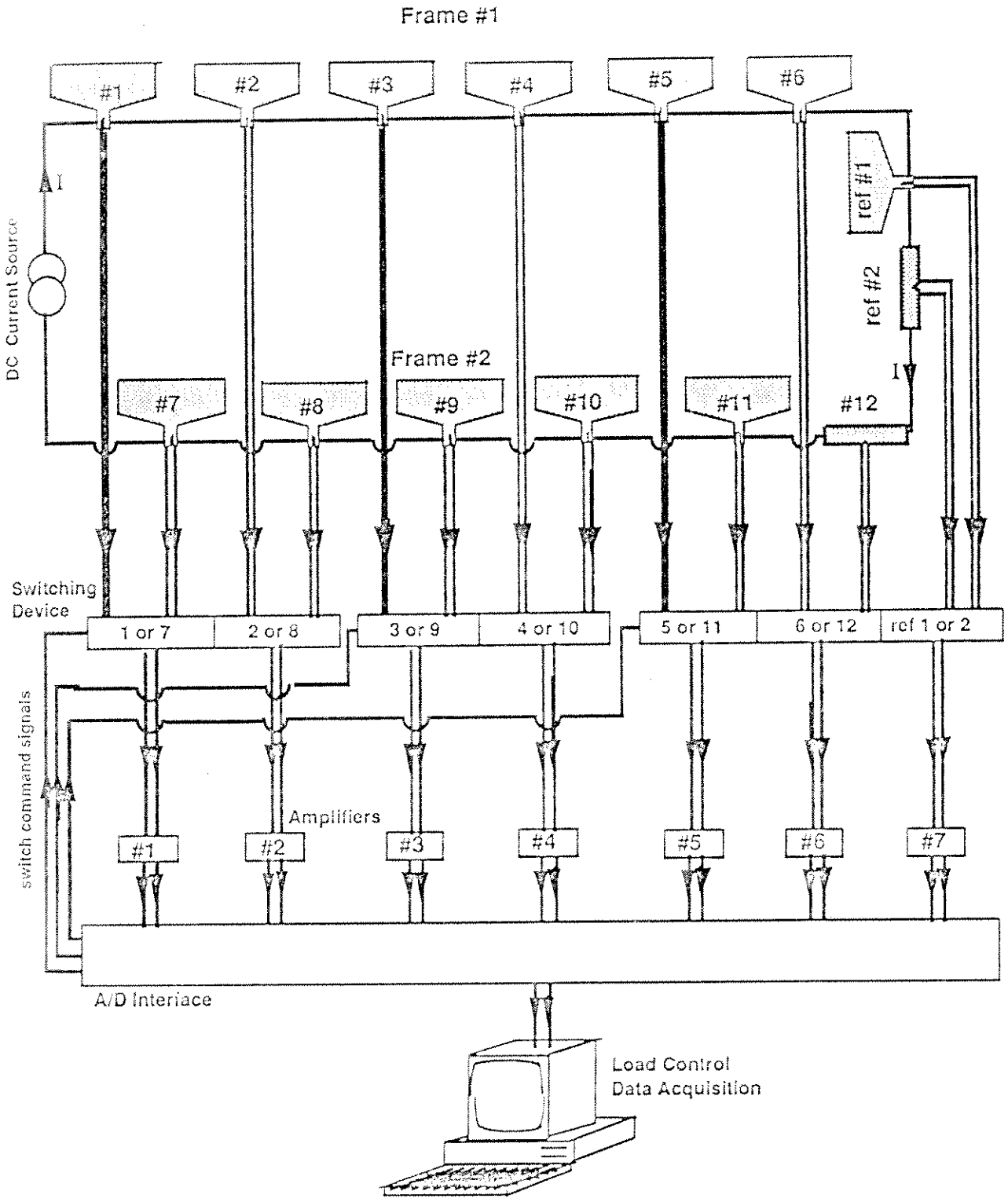

Figure 14—Schematic Diagram of the DC Potential System.

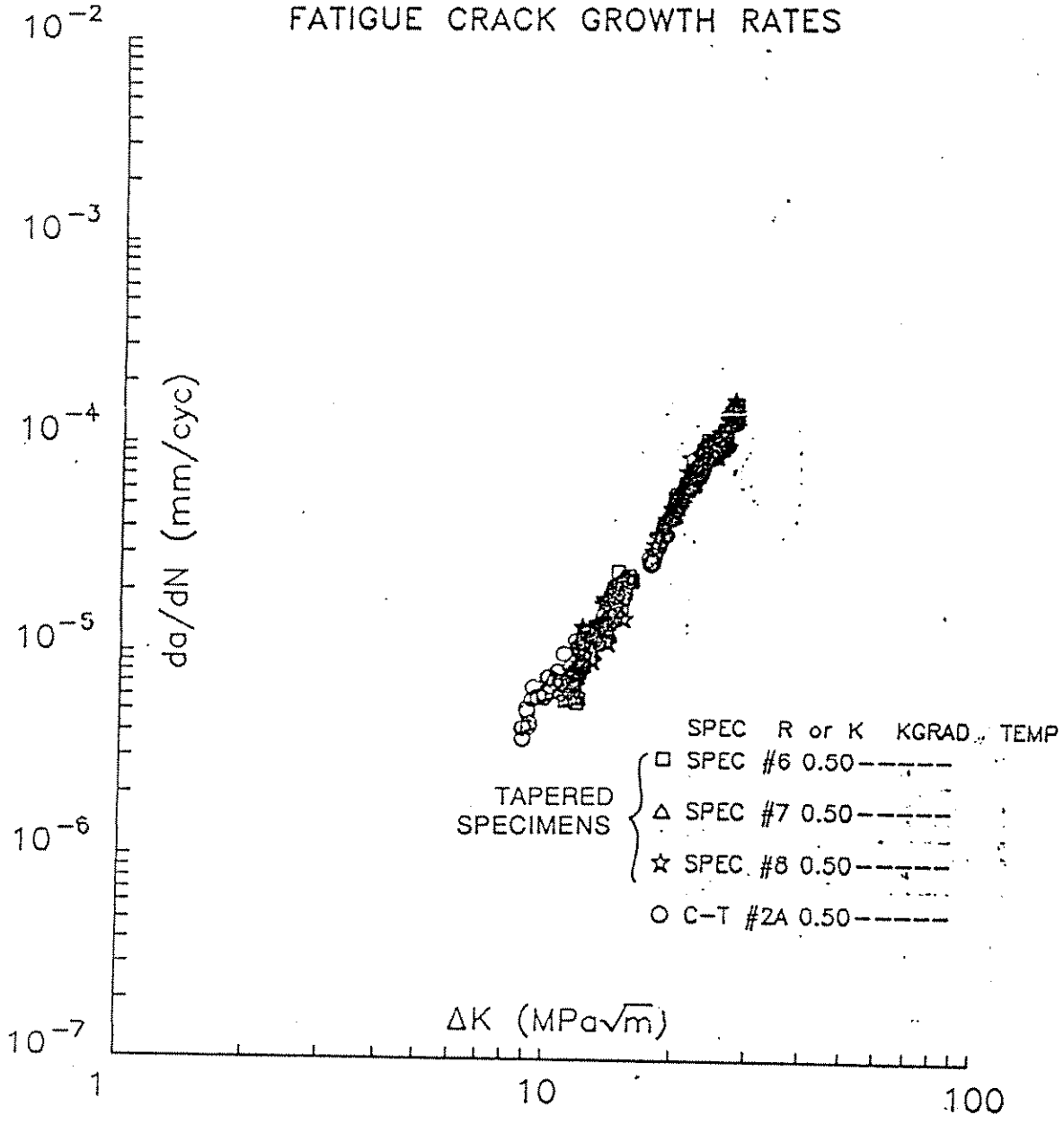

Figure 15—Comparison Between Tapered Specimen and C-T Specimen Results at R = 0.50.

CONCLUSION

The use of several specimens loaded in series in association with a computer assisted acquisition system increases the amount of data obtained in a given period of time, provided that the specimens respond to cyclic loading in a manner that is independent of one another. This condition is achieved by using tapered specimens instead of standard compact-tension specimens. The proposed procedure is particularly appropriate for low frequency, long-life situations, such as are associated with offshore structures, where determination of a single da/dN-ΔK curve might otherwise require a minimum of several months.

Several relatively new grades of high strength steels (yield stress 480–550 MPa) which are critical to innovative deep water structure concepts are now being tested in air and seawater using this multiple specimen technique. Fatigue crack growth characteristics in terms of ΔK, corrosion potential, stress ratio and microstructure are expected to be deduced in the near future. From this it is anticipated that design and materials selection for deep water structures can be carried out more efficiently and with greater confidence than would otherwise be possible.

REFERENCES

Paris, P.C., Bucci, R.J., Wessel, E.J., Clark, W.R., Mager, T.R., 1972, Stress Analysis and Growth of Cracks: STP 513, ASTM, Philadelphia, p. 141–176.

_____ 1986, Standard Test Method for Measurement of Fatigue Crack Growth Rate: E647A, Annual Book of ASTM Standards, American Society of Testing and Materials, Philadelphia.

Johnson, H.H., 1965, Calibrating the Electric Potential Method for Studying Slow Crack Growth: Materials Research and Standards, Vol. 5, No. 9, p. 442–445, September.

Schwalbe, K.H., Hellman, D, 1981, Application of the Electrical Potential Method to Crack Length Measurements Using Johnson's Formula: Journal of Testing and Evaluation, JTEVA, Vol. 9, No. 3, p. 218–221, May.

Hicks, M.A., and Pickard, A.C., 1982. A Comparison of Theoretical and Empirical Methods of Calibrating the Electrical Potential Drop Technique for Crack Length Determination: International Journal of Fracture Mechanics, Vol. 20, p. 91–101.

Watt, K.R., 1980, A Consideration of an A.C. Potential Drop Method for Crack Length Measurement: The Measurement of Crack Length and Shape During Fracture and Fatigue, C.J. Beevers Ed., p. 202.